Laser photothermolysis of single blood vessels in the chick chorioallantoic membrane (CAM)

Sol Kimel, Lars O. Svaasand, Thomas E. Milner, Marie Hammer-Wilson, Michael J. Schell, J. Stuart Nelson, and Michael W. Berns

Beckman Laser Institute and Medical Clinic (TEM, MHW, JSN and MWB) and Department of Medicine (MJS), University of California, Irvine, California, U.S.A.;
Department of Chemistry (SK), Technion-Israel Institute of Technology, Haifa, Israel;
Division of Physical Electronics (LOS), University of Trondheim, Trondheim, Norway

ABSTRACT

Individual blood vessels in the chick chorioallantoic membrane (CAM) were selectively coagulated through photothermolysis, using pulsed laser irradiation at 585 nm. Pulse durations were chosen to be 0.45 ms and 10 ms, which correspond to the thermal relaxation times in blood vessels of 30 μm and 150 μm diameter, respectively. The short pulses, at an energy density (or light dose) D=3 Jcm^{-2}, caused permanent occlusion of vessels of 40 μm diameter or less, while larger caliber vessels (60-120 μm) required D=4-5 Jcm^{-2}. The long-duration pulses, at D=7 Jcm^{-2}, caused coagulation of the larger diameter vessels; the small caliber vessels and capillaries showed resistance to photothermolysis and required multiple exposures to achieve coagulation. The dose vs diameter (D vs d) relationship for coagulation was calculated for the two pulse shapes. The energy deposited in a cylindrical absorber of diameter d by an optical field, incident perpendicular to the vessel, was expressed analytically and compared with the energy required to coagulate a blood vessel of the same lumen diameter. When thermal diffusion is incorporated into the model, our findings can be accounted for quantitatively. This information will be of use for improving the laser treatment of port wine stains and other vasculopathies. A surprising observation was that arterioles were damaged at lower incident energy densities than venules having the same lumen diameter, despite the fact that absorbance in oxygen-rich and oxygen-poor blood is the same for 585 nm radiation.

1. INTRODUCTION

The objective of this study is to gain an understanding of the biophysical principles underlying permanent coagulation of blood vessels, through conversion of selectively absorbed radiant energy into thermal energy. Such understanding is of importance in dermatological laser treatments, such as port wine stains (PWS)[1,2,3,4], telangiectasias[5,6], or hemangiomas[7] and may also be of benefit in the treatment of choroidal neovascularization[8,9].

The chick chorioallantoic membrane (CAM) is an established *in vivo* model for studying vascular effects[10]. The CAM vasculature is located in a transparent matrix[11] which allows direct visualization of blood flow as well as real-time observation of photothermal effects on blood vessels, such as vessel dilation, constriction, hemostasis and rupture. The CAM matrix does not significantly absorb or scatter radiation. Thus, the influence of pertinent laser parameters (wavelength, pulse duration and energy density) can be studied conveniently. Moreover, the CAM is a self-contained system which lends itself to mathematical modeling of optical and thermal effects[12]. Preliminary considerations are presented here for the choice of laser parameters, which are fully described in the Materials and Methods section.

1.1. Wavelength (λ)

In the transparent CAM, light anywhere within the visible spectrum may be used to irradiate the blood vessels, without encountering absorption in overlying epidermis which normally accompanies irradiation of dermal tissues[13,14]. The absorption of blood in the yellow-red spectral region around 585 nm was chosen for irradiation, in accordance with general considerations associated with increased light penetration in tissue at longer wavelengths[1,14,15,16]. A singular feature of the CAM is the possibility to study coagulation patterns in individual arterioles and venules. We seek, therefore, to equalize photothermal effects due to light absorption by the two endogenous chromophores, oxyhemoglobin (HbO_2) and hemoglobin (Hb). Equal absorption is achieved at the isosbestic point (λ=585 nm) in the absorption spectra of these two target chromophores. Because of deeper tissue penetration, this wavelength is of clinical interest, even though the absorption coefficient at 585 nm is 50% lower than the absorption peak of HbO_2 at λ=577 nm[15,16].

0-8194-1344-5/94/$6.00

1.2. Pulse duration (t_p)

The pulse duration governs the spatial confinement of the thermal energy within the targeted vessel[1,17]. Ideally, the pulse duration (t_p) should be compatible with the diameter (d) of the vessel and be about equal to the thermal relaxation time (τ_d) for that dimension ($\tau_d=d^2/16\chi$, where χ is the thermal diffusivity). This is defined as the time required for the instantaneous temperature, generated inside the target after exposure to the laser pulse, to decrease by 50% (see Discussion). Taking $\chi=1.4\times10^{-7}$ m^2s^{-1}, typical values for τ_d are 0.2 ms for d=20 μm and 4.5 ms for d=100 μm. If $t_p>>\tau_d$, heat diffuses outside the vessel during the laser exposure, reducing the target specificity, and can cause additional thermal damage to surrounding tissue. A very short pulse, $t_p<<\tau_d$, will generate a high-peak intravascular temperature rise, leading to localized explosive vaporization of tissue water, or to photoacoustic transients which will result in vessel rupture[18]. In such cases, repair mechanisms may revascularize the tissue[1].

1.3. Pulse energy density (D)

For PWS therapy, it is important to know the damage threshold dose in hypervascular skin, $D_{th}(t_p)$, sufficient to effect selective thermal injury to vessel wall structures, without causing rupture of the targeted vessel. The magnitude of $D_{th}(t_p)$ is difficult to establish by theoretical modeling, because of epidermal melanin absorption, multiple scattering events within the skin, and the fact that blood vessels are located at different dermal depths[16]. In the CAM, scattering and nonspecific absorption are small and measurements are made on identifiable targets. The depth of the targeted vessel in the CAM is of little consequence, provided no other superficial vessel is seen to shield part of the incident beam. Thus, measurements in the CAM will provide single-vessel values of the damage threshold dose, $D_0(d,t_p)$, which can be used as input in the derivation of the threshold value for the composite vasculature, $D_{th}(t_p)$.

2. MATERIALS AND METHODS

2.1. Laser parameters

A continuous wave (CW) Ar-ion pumped dye laser (model 920, Coherent, Palo Alto, CA) was used for single-vessel irradiation. The laser delivered a maximum power of 1.4 W at 585 nm, as measured with a power meter (model 210, Coherent). The laser beam was transmitted through an 80 μm core-diameter multimode fiber terminated with an adjustable focusing microlens positioned in a hand piece. The diameter of the beam at the focus was 500 μm, giving an energy density of $700t_p$ (Jcm^{-2}). The CW laser was pulsed with a foot pedal controlled mechanical shutter; the pulse duration was preselected at the shortest attainable setting of t_p=10 ms. The resulting energy density D = 7 Jcm^{-2} was marginally sufficient to cause injury and vessel damage was observed to occur only in the beam center (spot size ≈ 200 μm).

A flash lamp-pumped dye laser (model SPTL-1, Candela, Weyland, MA) was used for multiple-vessel irradiation. The laser was tuned to λ=585 nm and delivered pulses of duration t_p=0.45 ms. The beam was coupled into a 1 mm core-diameter multimode fiber terminated with a microlens that focused the laser output to a 5 mm diameter circular spot of uniform light intensity. The optical energy exiting the fiber was varied between 0.7 and 1.3 J, as measured with a calibrated energy meter (Ophir, model 10A-P), giving energy densities on the CAM membrane ranging between D = 3 and 6 Jcm^{-2}.

2.2. Preparation of intact CAMs

The protocol for CAM preparation was a modification of a previously described technique[10]. Fertilized eggs (Hy-line W36 white leghorn) were washed with 70% alcohol, incubated at 37 °C in 60% humidity, and rolled over hourly. On day 3-4 of embryonic development, a hole was drilled in the apex and 2-3 ml albumin was aspirated from each egg to create a false air sac. On the following day, part of the CAM was exposed by opening a round window of 20 mm diameter in the shell which was covered with a Petri dish. The eggs were placed in a stationary incubator until the CAM was fully developed and ready for experimentation. On day 10-12, sterile teflon O-rings (6.2 mm inner diameter, 9 mm outer diameter and 1.4 mm annular width) were placed on the surface of the CAM, each demarcating a location where individual blood vessels and capillaries were clearly visible and to which the laser beam

was directed. A drop of normal saline was added within the ring area to reduce spurious light reflection and to prevent desiccation of the CAM during the experiment[12]. Outside of the incubator, eggs were kept at 37 °C in a heating block filled with glass beads. At the time of irradiation, the CAM was illuminated with a cold white-light fiber optic source (Volpi, Intralux, model 100 HL) and placed under a stereomicroscope (Olympus, model SZH), equipped with a video camera (Panasonic, model AC-2510), giving a total magnification of 70x on a color monitor (Sony, model KV-1393R).

2.3. Vessel Selection

It was convenient to subdivide the extensive microvascular network of the CAM according to the following branching pattern[19]. The capillaries served as a reference and were designated vessels of "order-0". The smallest precapillary vessels (arterioles - a) as well as the smallest postcapillary vessels (venules - v) were assigned "order-1". The convergence of two order-1 vessels was assigned as an "order-2" vessel and similarly two order-2 vessels formed an "order-3" vessel. Table I presents, for each order, the mean number N of blood vessels per cm^2, the mean vessel length l (μm) and diameter d (μm) in a mature CAM at day 10[19]. The CAM area, viewed at a magnification 70x on the monitor during laser irradiation had a diameter of 3 mm and typically comprised 1-2 vessels of order-3, six of order-2 and approximately fifteen of order-1; these were about equally divided between precapillaries (a) and postcapillaries (v). The mean number of vessels in the capillary bed (order-0) in the field of view, at the magnification used, was estimated to be one hundred.

2.4. Irradiation Procedures

The long-pulse laser was used for precise microspot irradiation of individual target vessels of a given type (a or v) and order (1, 2 or 3). Focusing adjustment and diameters of specific vessels to be irradiated were ascertained *in situ* by videotaping the field of view with the aiming beam in place and comparing it with the 1.4 mm annular width of the teflon ring. Laser exposures were performed under standard conditions: t_p = 10 ms, spot size 200 μm, and D= 7 Jcm^{-2}. Each vessel was exposed 3 times at the same site, keeping the time interval between sequential exposures to 30 s, so that the subsequent irradiation interacted with a vessel that had cooled down to ambient temperature and in which the exposed blood had been replaced. Repeated exposures caused cumulative thermal damage to the vessel wall, eventually leading to occlusion or, inadvertently, to hemorrhage (when the exposures were stopped).

The short-pulse laser was used to irradiate a field of vessels located inside a teflon ring on the CAM. The energy densities ranged from a sub-threshold-damage dose D=3 Jcm^{-2} to D=6 Jcm^{-2}, in 0.5 Jcm^{-2} increments. Each field was irradiated with a series of three laser pulses at 30 s intervals, unless hemorrhage occurred in an order-1 or higher-order vessel following the first or second exposure - at which point irradiation was stopped. When irradiating additional fields in the same CAM, care was taken to assure that the arterial and venous trees were not compromised by the previous exposures in an adjacent field.

After laser irradiation, the eggs were covered and returned to a stationary incubator. Selected specimens (among those that had not undergone massive hemorrhage) were inspected 24 h later for re-perfusion of the vessels.

2.5. Damage assessment and statistical analysis

The laser-induced vascular damage was graded as follows:

0 - no observable damage
1 - slight damage - vasodilation/constriction; temporary occlusion
2 - moderate damage - permanent occlusion
3 - severe damage - capillary extravasation; hemorrhage.

Stepwise logistic regression analysis[20] was used to assess the statistical significance of vessel type (arteriole vs venule), vessel order (1 vs 2 and 3; 1 and 2 vs 3) and energy level (for the short-pulse laser only). The two dependent variables analyzed were the number of exposures to any vessel damage (grade > 0) and the number of exposures to moderate or severe damage (grade > 1). When occlusion or hemorrhage occurred after 1 or 2 pulses, irradiation was stopped. For the short-pulse irradiation, this resulted in some vessels in the same exposure field which were not graded at all three exposures.

3. RESULTS

3.1. Long-pulse laser

Order-1 vessels had significantly less damage compared to higher order vessels (p=.0001). Forty-three percent of order-1 vessels were damaged after a single pulse compared to 75% for vessels of order-2 or 3; this differential was preserved after additional exposures (Figure 1). Arterioles were significantly more sensitive to moderate or severe damage than venules (p = .001). Fifteen out of 89 (17%) arterioles sustained moderate or severe damage after three exposures. By contrast, only 3/102 (3%) of the venules sustained comparable damage.

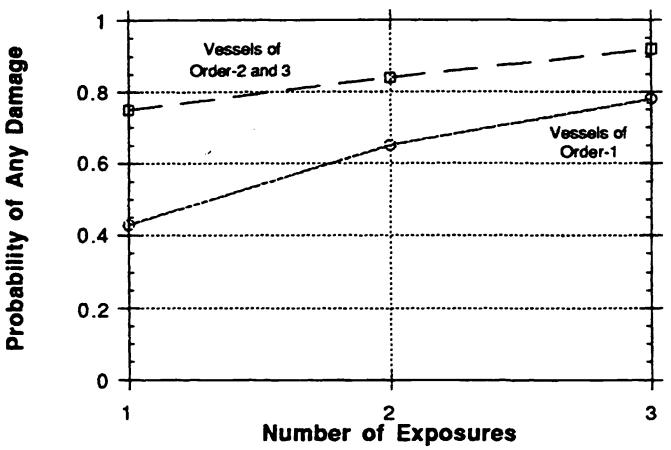

Figure 1: Probability of any vessel (arteriole or venule) damage (grade 1, 2 or 3) vs. number of long-pulse (t_p = 10 ms) exposures.

3.2. Short-pulse laser

Order-1 vessels were most sensitive to damage, vessels of order-3 were most resistant. Arterioles were more sensitive than venules and higher energy exposures resulted in more damage. Upon multiple exposures, injury first occurred to the capillary system, next to arterioles a1, and then to vessels a2 and v1. All p-values were less than .0001.

Figures 2a and 2b show the percentage of arterioles and venules with any (grade > 0) damage and with moderate or severe (grade > 1) damage, respectively, after 1, 2 and 3 exposures. Notably arterioles of order-3 have a similar damage profile as venules of order-2; nearly all arterioles of order-1 are damaged after a single exposure. Figures 2c and 2d show the effect of energy density on vessel (arterioles and venules) damage.

All damage to capillaries (less than order-1) was graded as either moderate or severe. Of 159 capillaries, 49 (31%) were damaged after one pulse, 6 additional capillaries (4%) were damaged on the second exposure and 2 (1%) were damaged on the third exposure; 102 (64%) were not damaged. Laser energy density was not statistically correlated with capillary damage.

4. DISCUSSION

4.1. Absorption by a cylindrical vessel in a uniform optical field

Consider a cylindrically shaped blood vessel, with outer diameter d and inner (lumen) diameter d_i, lying along the y-direction and exposed over length l to a pulsed, collimated light beam propagating in the z-direction as illustrated in Fig. 3. For convenience, it is assumed that the diameter of the beam (and thus l) is larger than d. Denaturation of the vessel wall occurs through heat conducted from the erythrocytes which have absorbed incoming light.

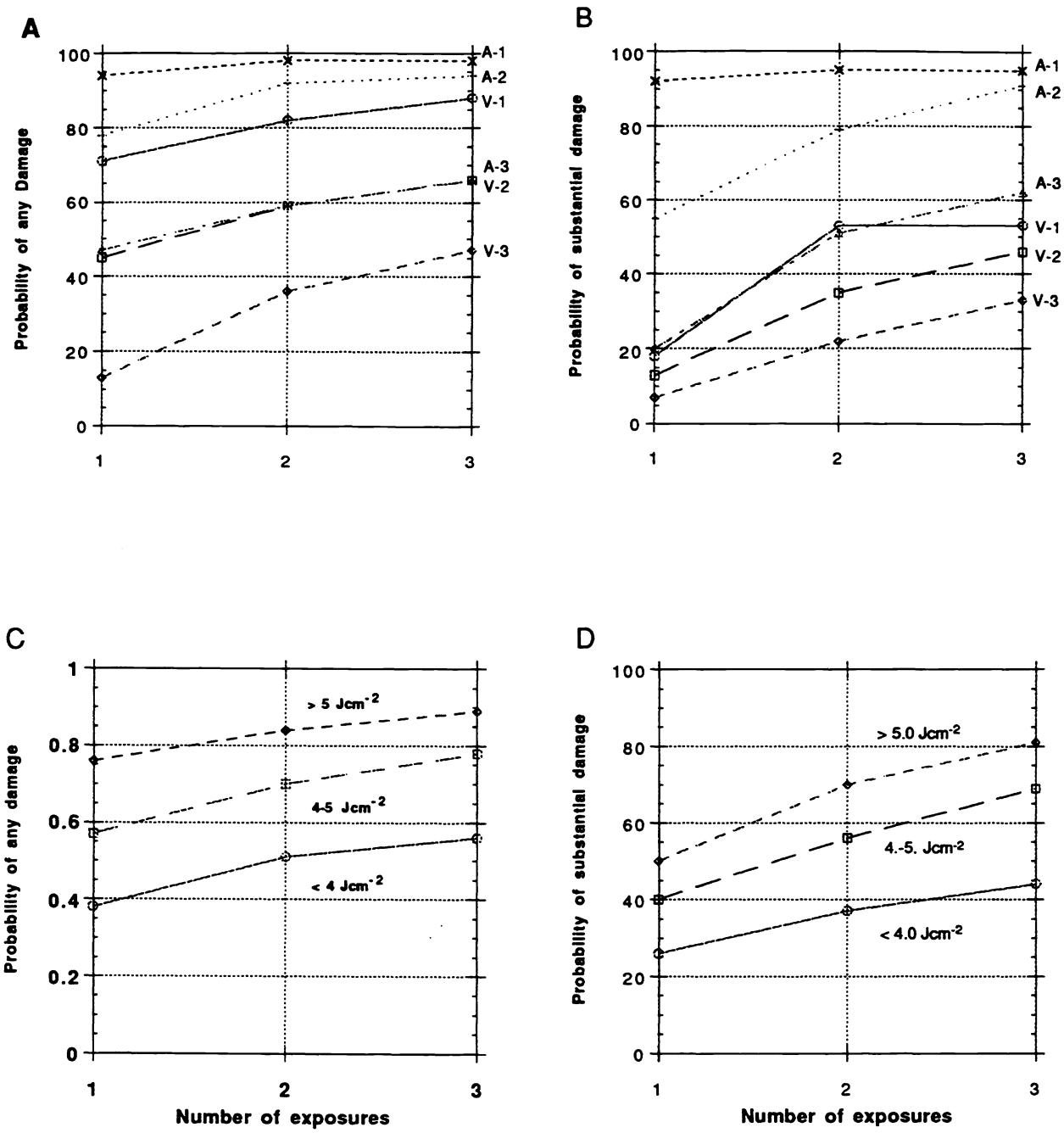

Figure 2: Probability of laser damage vs. number of short-pulse (t_p = 0.45 ms) exposures.

Panel A: Probability of any damage (grade 1, 2 or 3) to arterioles and venules of orders-1, 2, and 3.
Panel B: Probability of moderate or severe damage (grade 2 or 3) to arterioles and venules of order 1, 2, and 3.
Panel C: Probability of any damage to all vessel types (arterioles or venules of any order) versus incident laser energy density.
Panel D: As panel C, for moderate or severe vessel damage.

To a first approximation, the energy q required for thermally induced coagulation of blood in a vessel of unit length is given in equation 1

$$q/l = c\rho\pi(d/2)^2(T_f - T_i) \tag{1}$$

Here ρ is the mass density (gcm^{-3}) and c is the specific heat of blood (4.2 $Jg^{-1}K^{-1}$) taken to be equal to the corresponding values for water; T_i and T_f denote, respectively, the temperature before (35 ^0C) and immediately after the laser pulse. The critical temperature at the vessel wall required for coagulation of blood vessels is expected to be higher than that causing transient hemostasis (T_f= 70 ^0C)[21] and has to be maintained over relatively long times (>0.01 s) at hyperthermic conditions[13,22]. In the sample calculations of q presented in Table II we have assumed T_f =90 ^0C. When considering long-pulse microspot irradiation, values of q in Table II should be corrected for the cooling effect of blood flow in the axial direction during the time t_p[23]. Measured flow velocities (v) in the CAM vessels ranged from v=0.7 mms^{-1} when d=40 μm to v=1.4 mms^{-1} when d=100 μm[12]. For example, during t_p=10 ms, the blood flow in a vessel of l=200 μm and d=100 μm replaces about $t_p v/l$ =7% of the total volume in the exposed part of the vessel and q is correspondingly larger (neglected in Table II). Perfusion is even less important with short-pulse exposure since t_p is 20 times shorter and l is generally much larger than in the long-pulse microspot exposure. The cooling effect due to thermal diffusion at the vessel periphery will cause a non-uniform spatial distribution of temperature within the vessel, with a peak temperature in the center of the vessel (displaced somewhat toward the upper part facing the light beam) and lower temperatures at the periphery of the vessel[24].

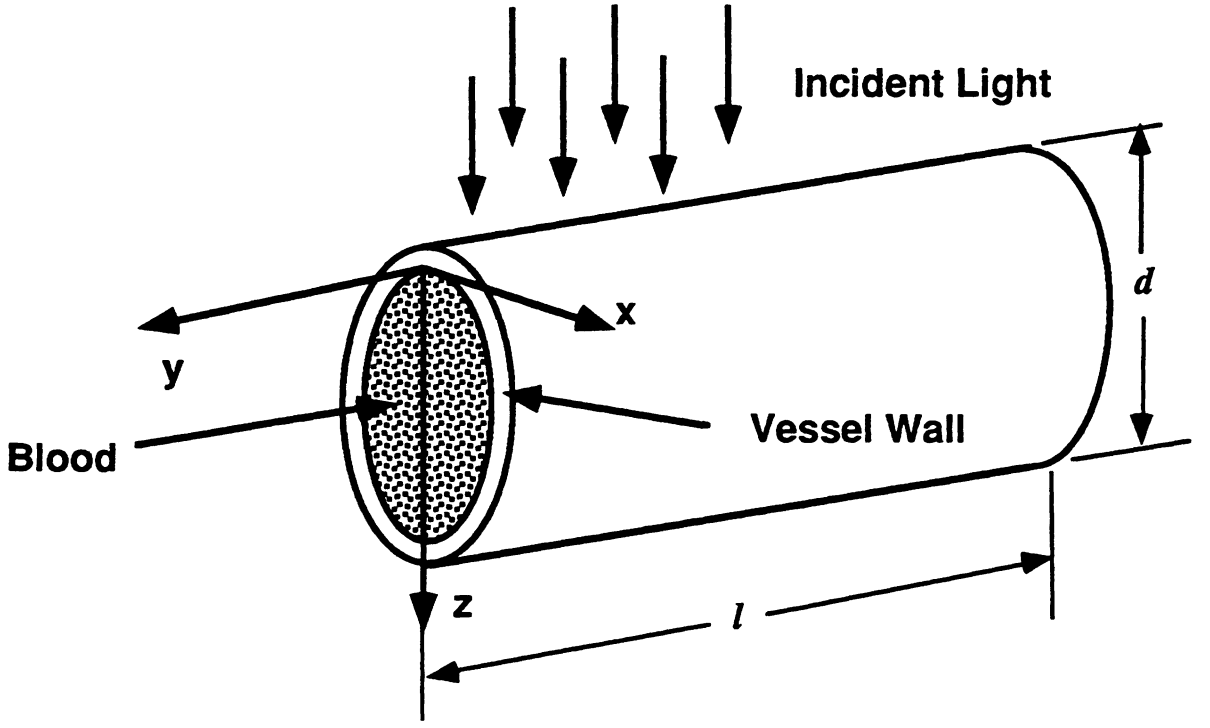

Figure 3: Coordinate geometry for calculation of light absorption in a vessel.

When we neglect light scattering and also reflections at the air/CAM and the CAM/vessel interfaces, the energy per pulse, Q_A, deposited in a blood vessel due to absorption from a uniform optical field, can be expressed analytically. In a cylindrical vessel of lumen diameter d_i and length l the net absorbed energy is

$$Q_A = \int_0^l dy \int_{-d_i/2}^{d_i/2} dx \int_0^{2\sqrt{(d_i/2)^2 - x^2}} D\alpha e^{-\alpha z} dz$$

$$= (\pi/2) D l d_i [I_1(\alpha d_i) - L_1(\alpha d_i)] \tag{2}$$

Here D (Jcm^{-2}) is the incident energy density; ld_i is the target area intercepting the light beam; $\alpha = \alpha(\lambda)$ is the absorption coefficient of blood; I_1 and L_1 are, respectively, the first-order modified Bessel and Struve functions[25]

which have been tabulated[26]. In order to visualize the role of αd_i on Q_A we reformulate Eq.2 in terms of the dimensionless variable $u=(1-x^2/r^2)^{1/2}$

$$Q_A = Dld_i \cdot \alpha d_i \cdot \int_0^1 e^{-\alpha d_i u}\sqrt{1-u^2}\,du \tag{3}$$

and plot $f = Q_A/Dld_i$ versus αd_i (see Fig. 4). The result represents the fraction of incident optical energy absorbed by the vessel and is completely general. It gives the fraction of energy absorbed by a cylinder containing a homogeneous absorber, e.g. blood for which α(585 nm)=170 cm^{-1} or α(577 nm)=430 cm^{-1} [16], or blood with added chromophores such as fluorescein or indocyanine green. Blood has a rather large absorbance at λ= 585 nm and for d_i > 100 μm (αd_i > 1.7) it can be seen (Figure 4) that more than 70% of the light incident on the upper surface of the vessel is absorbed. In Table II, Q denotes the energy absorbed by a blood vessel when irradiated with D=1 Jcm^{-2} at λ= 585 nm. The values show that for a blood vessel with a lumen diameter d_i = 20 μm, the coagulation energy q is equal to the energy intercepted by that vessel from an optical field having $D \geq 1.4$ Jcm^{-2}. When d_i = 120 μm, an incident energy density $D \geq 2.9$ Jcm^{-2} is predicted to effect coagulation.

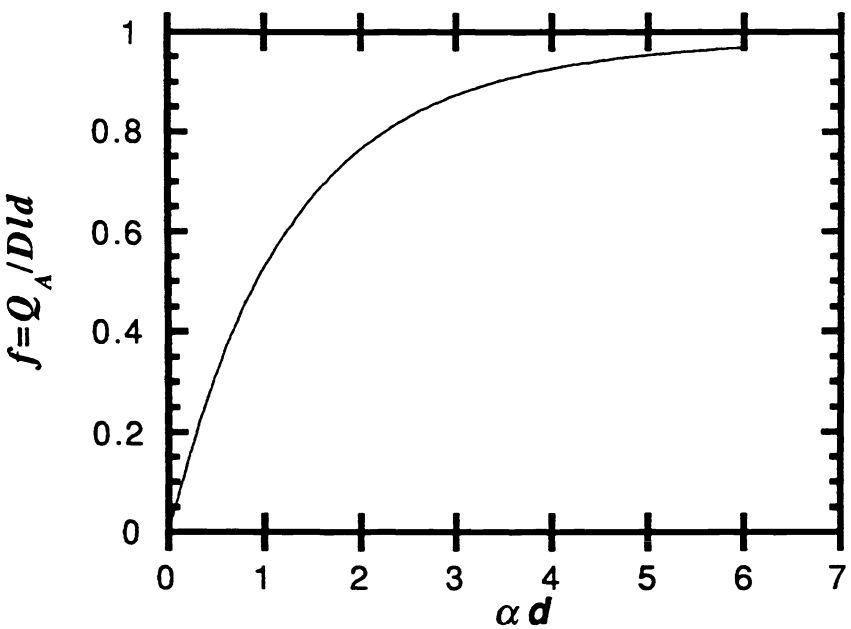

Figure 4: Fraction of incoming light absorbed by a homogeneous cylindrical volume with diameter d and absorbance α.

4.2. Effects of thermal diffusion

The effect of thermal diffusion out of the heated vessel into the surrounding tissue will now be considered. It is particularly relevant for small diameter vessels and/or long irradiation times, i.e. $t_p >> \tau_d = d^2/16\chi$. We make the ansatz that thermal energy diffuses out of a vessel in an exponential fashion, so that for t > t',

$$dQ(t,t') = dQ_A(t')e^{-(t-t')/\tau_d} \tag{4}$$

Here $dQ_A(t')$ denotes the incremental amount of optical energy absorbed in the exposed lumen during dt' at a time t'; $dQ(t,t')$ denotes the corresponding thermal energy after the time interval (t-t'). The thermal energy remaining in the vessel at time t is found by integrating Eq. (4) over the duration of the laser pulse, $0<t'<t_p$. The result is

$$Q_t = Q_A(\tau_d / t_p)[1 - e^{-t/\tau_d}], \quad t \geq t_i \tag{5a}$$

$$= \Delta T c \rho l \pi (d/2)^2 \tag{5b}$$

Since we are interested in the coagulation temperature of the entire vessel (i.e. lumen and vessel wall) d in Eq. (5b) is taken to be the outer diameter of the vessel. After inspecting histologic sections of our CAM preparations, we established that $\langle d_i \rangle = 0.93\langle d \rangle$ for venules and $\langle d_i \rangle = 0.88\langle d \rangle$ for arterioles, with smaller vessels (capillaries or order-1) having relatively thicker walls. Taking as an average $d_i = 0.9d$, we use in Eq. (5b) for the specific heat of the vessel

$$c\rho = 4.18(d_i/d)^2 + 3.50[1-(d_i/d)^2] = 4.05 \text{ Jcm}^{-3}\text{K}^{-1}$$

where 4.18 and 3.50 $\text{Jcm}^{-3}\text{K}^{-1}$ are, respectively, the specific heat of the lumen and vessel wall cellular materials and the mass density is taken to be $\rho = 1$ gcm^{-3}.

In Figure 5 we have plotted the temperature rise ΔT given by Eq. (5b) for the long-pulse laser ($t_p = 0.01$s and $D = 7$ Jcm^{-2}) and for the short-pulse laser ($t_p = 0.45$ ms and $D = 3$ Jcm^{-2}). For the two curves in Figure 5 a striking feature is the different dependence of ΔT on the vessel diameter d. The long-pulse exposure causes a monotonic temperature rise with d over the given range $d < 130$ μm. At larger d the temperature rise will reach a maximum and, eventually, decrease as $1/d$. In contrast, the temperature rise due to the short-pulse exposure reaches its maximum at a smaller diameter. Consequently, for a critical temperature $T_f = 90$ °C ($\Delta T = 55$ °C), Figure 5 indicates that the short-pulse exposure affects predominantly small diameter vessels (of order-1 and -2) whereas the long-pulse exposure will damage the larger diameter vessels.

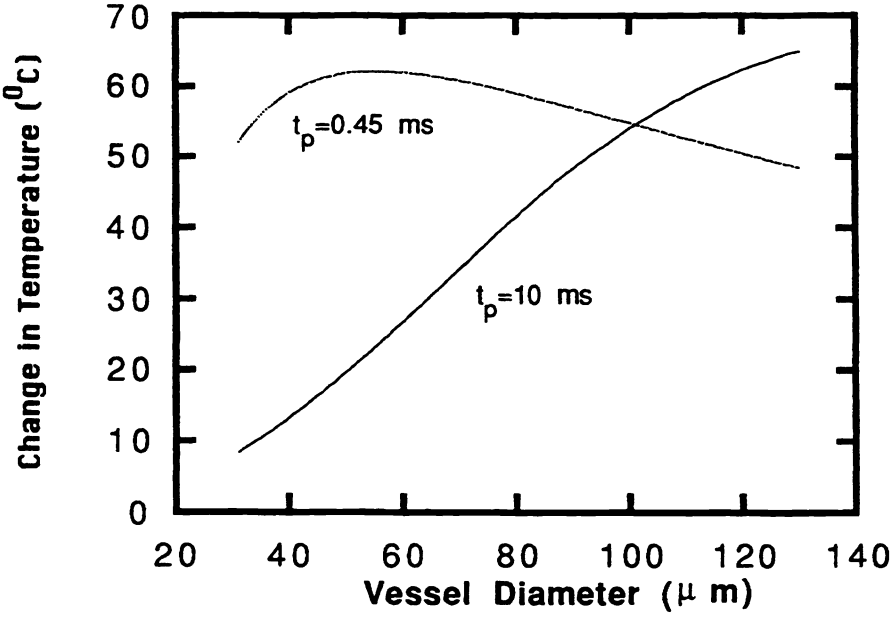

Figure 5: Change in vessel temperature for short and long-pulse laser irradiation.

4.3. Instantaneous temperature increase inside an absorbing cylinder

For a short laser pulse ($t_p << \tau_d$), $Q_t \approx Q_A$ (in Eq. 5a). The absorbed optical energy gives rise to a non-uniform temperature distribution in the lumen

$$\Delta T(x,z,t_p) = (1/c\rho)\frac{dQ_A}{dV}(x,z) = (D\alpha/c\rho)e^{-\alpha z(x)} \tag{6}$$

where dQ_A/dV is the absorbed energy density (Jcm^{-3}) and the other parameters are as defined in Eqs. 1,2. Upon substituting z(x), as defined in equation 7 (see Fig. 3),

$$z(x) = z - d/2 + \sqrt{(d/2)^2 - x^2} \tag{7}$$

into Eq. 6 the spatial distribution of the temperature rise in the lumen is obtained. In Fig. 6, the cross sections of vessels of order-1, 2 and 3 with (see Table I) d = 50, 80, and 110 μm, respectively, are diagrammed. Inside each diagram are plotted the isotherm curves (ΔT = 55 °C) for D = 3 and 5 Jcm^{-2}. The curves define the transition zones between damaged ($T_f > 90$ °C) and non-damaged ($T_f < 90$ °C) lumen volume. It is evident that smaller caliber vessels are more easily coagulated than larger ones. According to the hemodynamic criterion, total occlusion occurs when at least 61% of the lumen has coagulated, i.e. the critical temperature $T_f = T_i + 55$ K = 90 °C reaches half way through the vessel diameter[16].

Also, we note that at the lowest energy density (D = 3 Jcm^{-2}) only the small diameter vessels show thrombosis (>61% of lumen has coagulated), whereas at D = 5 Jcm^{-2} the small and medium vessels will have coagulated completely while the larger vessels of order-3 will show partial occlusion. This behavior is borne out by by the results for the short-pulse laser presented in Fig. 2.

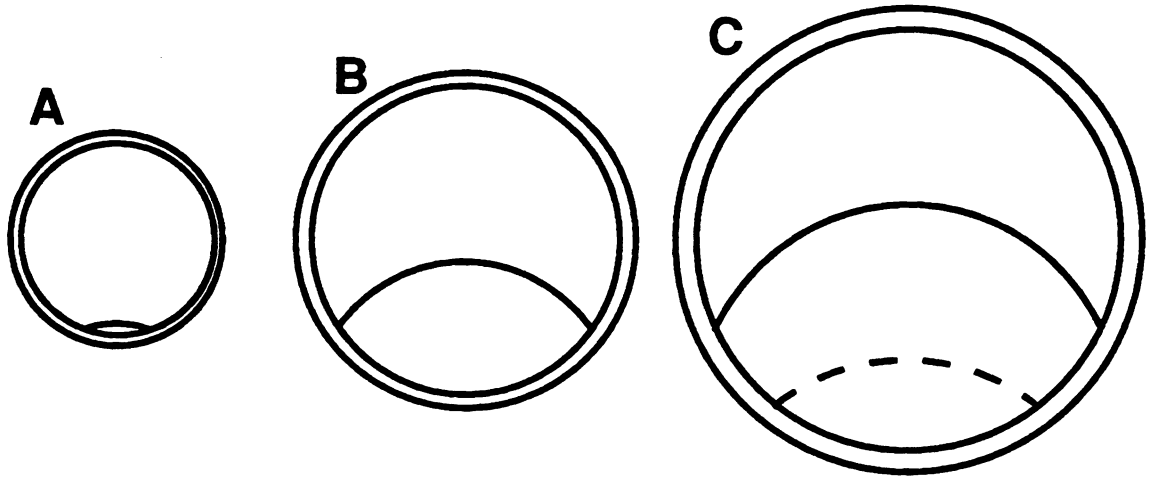

Figure 6: Isotherm curves (ΔT=55°C) in vessels of various diameters (d) and incident energy densities (D). A: d=50 μm and D=3 Jcm^{-2} ; B: d=80 μm and D=3 Jcm^{-2} ; C: d=110 μm and D = 3 (——) or 5 (– – –) Jcm^{-2}.

4.4. Long-pulse photothermolysis

For the long-pulse exposures the results given above must be modified to include the full effects of thermal diffusion. This situation has been modeled mathematically[16,24,27,28] but is beyond the scope of this discussion. Our main aim has been to present analytical results which provide direct answers for single vessel exposure.

4.5. Arterial and venous response

One of the more salient phenomena observed in the present study was the higher vulnerability for thermal injury of arterioles as compared to venules. This occurred for the three vessel calibers considered and for both short-pulse and long-pulse exposures. In the CAM, arterial (oxygen poor) and venous (oxygen rich) blood possess equal light absorbance at 585 nm; thus, vessels of the same lumen diameter are expected to undergo similar thermal stress. In a study of prolonged heating of blood vessels it was reported that arteries showed less vasoconstriction (and faster

post-heating recovery) than veins[22]. This is at variance with our observations. A possible explanation of our findings might be based on considerations of vascular anatomy. The arteriolar walls consist of three concentric layers: an endothelial tube, an intermediate layer of smooth muscle cells, and an outer coat of fibrous elements. The thickness of the arteriolar wall varies with vessel caliber and function; the walls of venules are always thinner than those of arterioles of equal caliber. When this difference is significant, a comparison of thermal damage may be made between arterioles of "order-n" and venules of "order n-1". However, in the CAM the difference in vascular cross section is generally small. If we take as typical wall thicknesses $0.06d$ and $0.035d$ for arterioles and venules, respectively, the ratio for the lumen volume of arterioles and venules for two vessels with the same outer diameter will be $(0.88/0.93)^2=0.9$. This ratio is too close to unity to explain our observations. Moreover, contrary to the observations, the long-pulse laser would then be expected (see Fig. 5) to damage preferentially the venules, while the short-pulse laser would preferentially damage the arterioles.

Another point of difference is the platelet aggregation initiated by the chain of biochemical reactions triggered by thermal trauma, which is different in arterioles and venules. This seems to be consistent with reports of PDT-induced vasoconstriction, where it was shown that 90% of the arterioles were affected by photochemical injury versus 70% of the venules[29]. However, on the time scale of photothermolysis ($t \approx 10$ ms) no platelet aggregation is expected to occur in real time.

Finally, it should be noted that blood clots can be transported downstream in venules, but not in arterioles since they get blocked in the capillaries. This difference in permanent clotting is a component in our interpretation for the lower threshold for arteriolar photothermolysis.

In conclusion, this study described the first controlled experiment of photothermolysis in single blood vessels *in vivo*. The observations of damage threshold vs vessel diameter were quantified. They were interpreted using a theoretical model which has wide applicability to a number of vasculopathies.

5. ACKNOWLEDGMENTS

This work was supported by Department of Energy grant DE-F603-91ER61227; Office of Naval Research grant N00014-91-C-0134; Biomedical Resource Technology Program grant RR01192, and grant 0088-308 from the US-Israel Binational Science Foundation. JSN is the recipient of a Dermatology Foundation Career Development Award. Jeffrey J. Andrews and Glen A. Profeta provided laser technical support.

6. REFERENCES

1. R.R. Anderson and J.A. Parrish, "Selective photothermolysis: Precise microsurgery by selective absorption of pulsed radiation", *Science*, 220, 524-527 (1983).

2. J.M. Garden, O.T. Tan, R. Kerschmann, J. Boll, H. Furumoto, R.R. Anderson and J.A. Parrish, "Effect of dye laser pulse duration on selective cutaneous vascular injury", *J. Invest. Dermatol.*, 87, 653-657 (1986).

3. J.M. Garden, L.L. Polla and O.T. Tan, "The treatment of port-wine stains by the pulsed dye laser", *Archiv. Dermatol.*, 124, 889-896 (1988).

4. J.S. Nelson and J. Applebaum, "Clinical management of port-wine stain in infants and young children using the flashlamp-pulsed dye laser", *Clin. Pediatr.*, 29, 503-508 (1990).

5. A. Orenstein and J.S. Nelson, "Treatment of facial vascular lesions with a 100-μm spot 577-nm pulsed continuous wave dye laser", *Ann. Plast. Surg.*, 23, 310-316 (1989).

6. J.M. Key and M. Waner, "Selective destruction of facial telangiectasia using a copper vapor laser", *Archiv. Otolaryngol - Head Neck Surg.*, 118, 509-513 (1992).

7. R. Ashinoff and R.G. Geronomus, "Capillary hemangiomas and treatment with the flash lamp-pumped pulsed dye laser", *Arch. Dermat.*, 127, 202-205 (1991).

8. N. Katoh, K. Takahashi, T. Itagaki, H. Okhuma, M. Uyama, "Choroidal vascular repair following orange dye laser photocoagulation", *Jap. J. Ophthalmol.*, 33, 166-172 (1989).

9. E. van der Zypen, F. Fankhauser, E.F. Luscher, S. Kwasniewska and C. England, "Induction of vascular haemostasis by Nd:Yag laser light in melanin-rich and melanin-free tissue", *Documenta Ophthalmologica*, 79, 221-239 (1992).

10. D. Knighton, D. Ausprunk, D. Tapper and J. Folkman, "Avascular and vascular phases of tumor growth in the chick embryo", *Brit. J. Cancer*, 35, 347-356 (1977).

11. A. Fuchs and E.S. Lindenbaum, "The two- and three-dimensional structure of the microcirculation of the chick chorioallantoic membrane", *Acta Anat.*, 131, 271-275 (1988).

12. S. Kimel, L.O. Svaasand, M. Hammer-Wilson, V. Gotfried, S. Cheng, E. Svaasand and M.W. Berns, "Demonstration of synergistic effects of hyperthermia and photodynamic therapy using the chick chorioallantoic membrane model", *Lasers Surg. Med.*, 12, 432-440 (1992).

13. R. Birngruber, F. Hillenkamp and V.P. Gabel, "Theoretical investigation of laser thermal retinal injury", *Health Phys.*, 48, 781-796 (1985).

14. M.J.C. van Gemert, A.J. Welch and A.P. Amin, "Is there an optimal laser treatment for port wine stains?", *Lasers Surg. Med.*, 6, 76-83 (1986).

15. O.T. Tan, S. Murray, A.K. Kurban, "Action spectrum of vascular specific injury using pulsed radiation", *J. Invest. Dermatol.*, 92, 868-871 (1989).

16. M.J.C. van Gemert, A.J. Welch, I.D. Miller, O.T. Tan, "Can physical modeling lead to an optimal laser treatment and strategy for port-wine stains?", in *Laser Applications in Medicine and Biology*, M.L. Wolbarsht, Ed., vol 5, pp. 199-275, Plenum Press, New York, 1991.

17. M.J.C. van Gemert and A.J. Welch, "Time constants in thermal laser medicine", *Lasers Surg. Med.*, 9, 405-421 (1989).

18. B.S. Paul, R.R. Anderson, J. Jarve and J.A. Parrish, "The effect of temperature and other factors on selective microvascular damage caused by pulsed dye laser", *J. Invest. Dermatol.*, 81, 333-336 (1983).

19. D.O. DeFouw, V.J. Rizzo, R. Steinfeld and R.N. Feinberg, "Mapping of the microcirculation in the chick chorioallantoic membrane during normal angiogenesis", *Microvasc. Res.*, 38, 136-147 (1989).

20. D.W. Hosmer and S. Lemeshaw, *Applied Logistic Regression*, John Wiley, New York, 1989.

21. A.L. McKenzie, "Physics of thermal processes in laser-tissue interaction", *Phys. Med. Biol.*, 35, 1175-1209 (1990).

22. W. Gorisch and K.P. Boergen, "Heat-induced contraction of blood vessels", *Lasers Surg. Med.*, 2, 1-13 (1982).

23. F. Fankhauser, H. Bebie and S. Kwasniewska, "The influence of mechanical forces and flow mechanisms on vessel occlusion", *Lasers Surg. Med.*, 6, 530-532 (1987).

24. J.W. Pickering, P.H. Butler, B.J. Ring and E.P. Walker, "Computed temperature distribution around ectatic capillaries exposed to yellow (578 nm) laser light", *Phys. Med. Biol.*, 34, 1247-1258 (1989).

25. I.S. Gradshteyn, I.M. Ryzhik (Ed., A. Jeffrey), *Table of Integrals, Series and Products*, Academic Press, San Diego, 1980.

26. Mathematical Tables Project, "Table of Struve Functions $L_V(x)$ and $H_V(x)$", *J. Math. Phys.*, 25, 252-259 (1946).

27. S.L. Jacques and S.A. Prahl, "Modeling optical and thermal distributions in tissue during laser irradiation", *Lasers Surg. Med.*, 6, 494-503 (1987).

28. L.O. Svaasand, "On the propagation of thermal waves in blood perfused tissues", *Lasers Life Sci.*, 2, 289-311 (1988).

29. M.W.R. Reed, T.J. Wieman, D.A. Schuschke, M.T. Tseng and F.N. Miller, "A comparison of the effects of photodynamic therapy on normal and tumor blood vessels in the rat microcirculation", *Radiation Res.*, 119, 542-552 (1989).

Table I The mean number N (per cm^2), the mean length l (μm) and the mean diameter d (μm) of blood vessels in the CAM at day 10 (after reference 19).

Vessel type	Vessel order	N	l (μm)	d (μm)
	3	16	1570	112
precapillary (artery)	2	57	740	71
	1	167	320	45
capillary	0			
	1	98	410	54
postcapillary (vein)	2	33	900	76
	3	15	1980	113

Table II Thermal relaxation times τ_d in blood vessels with lumen diameter d_i. The coagulation energy q for a vessel of unit length (1 cm) is compared with the optical energy Q absorbed when that vessel is exposed to pulsed light ($t_p << \tau_d$) at λ = 585 nm at an energy density D = 1 Jcm^{-2}.

Vessel Order	d_i (μm)	τ_d (ms)	q (mJ)	Q (mJ)
0	20	0.18	0.7	0.5
1	40	0.71	2.9	1.6
1	60	1.61	6.5	3.3
2	80	2.86	11.6	5.1
2	100	4.46	18.1	7.2
3	120	6.43	26.0	9.1
3	140	8.75	35.4	11.6